

# Characterization and Catalytic Activity of Bimetallic Pt-In/Al<sub>2</sub>O<sub>3</sub> and Pt-Sn/Al<sub>2</sub>O<sub>3</sub> Catalysts

Fabio B. Passos,\* Donato A. G. Aranda,†,‡ and Martin Schmal†,‡,1

\*Departamento de Engenharia Química, Universidade Federal Fluminense, R. Passos da Pátria, 156, Niterói, RJ, 24210-240, Brazil; †NUCAT/COPPE, Universidade Federal do Rio de Janeiro, Caixa Postal 68502, Rio de Janeiro, RJ, 21945-970, Brazil; and ‡Escola de Química, Universidade Federal do Rio de Janeiro, Caixa Postal 68542, Rio de Janeiro, RJ, 21940-900, Brazil

Received November 4, 1997; revised May 29, 1998; accepted June 1, 1998

Bimetallic platinum-indium and platinum-tin supported on alumina catalysts were investigated by temperature programmed reduction (TPR), hydrogen chemisorption, and UV-Vis diffuse reflectance spectroscopy (DRS). DRS results indicated that the interaction between Pt and In or Sn takes place during the reduction step. The TPR results showed that, after reduction at 773K, about 50–80% of indium and 25–50% of tin are in a zero-valent state in the bimetallic system, depending on the preparation method. Also, there is a partial shift of the reduction of In<sup>3+</sup> and Sn<sup>4+</sup> to the platinum precursor temperature range. The interaction between indium and platinum was also demonstrated by the decrease of platinum adsorption capacity, when indium was present. The use of model reactions were shown to be adequate to differentiate the effects of Sn and In on Pt/Al<sub>2</sub>O<sub>3</sub> catalysts. The turnover frequency for cyclohexane dehydrogenation, a structure insensitive reaction, was not affected by the presence of the promoter. In the case of reactions that require larger platinum ensembles to occur, the presence of the promoter caused a decrease in the turnover frequency, due to the dilution of platinum surface atoms with the promoter atoms. There was a larger decrease in the turnover frequency of the methylcyclopentane hydrogenolysis when In was used as promoter, indicating that In dilutes the Pt atoms more homogeneously than Sn. For the *n*-heptane conversion, the addition of In or Sn improved the stability of the catalysts, caused a decrease in the selectivity for hydrogenolysis, and an increase in the selectivity for dehydrogenation and aromatization products. The main difference between In and Sn was that Sn promoted a higher selectivity for isomerization products. © 1998 Academic Press

## INTRODUCTION

The wide application of supported platinum bimetallic catalysts in hydrocarbon conversions has led to intense research on this class of catalysts (1–3). Compared to the catalysts containing only Pt, bimetallic catalysts are more stable, more selective, and showed higher activity in the conversion of hydrocarbons. A change of bond strength

between chemisorbed hydrocarbons and Pt surface atoms due to electron transfer from the promoter to Pt (electronic effect) and a dilution of the Pt surface atoms to decrease the ensemble size by the second metal (geometric effect) have been proposed as reasons for the beneficial effect of the promoter.

In the case of dehydrogenation of long chain alkanes, a multimetallic Al<sub>2</sub>O<sub>3</sub> supported platinum catalyst containing In and Sn as promoters is employed (4). The addition of Sn to Pt/Al<sub>2</sub>O<sub>3</sub> catalysts has been investigated in several studies (5–10), while the effect of In received less attention (11). Recently, using calorimetric measurements of H<sub>2</sub> and CO adsorption on alumina supported Pt-Sn and Pt-In catalysts and infrared spectroscopy of adsorbed CO, it was observed that the main mechanism for modification of the platinum was geometric, with any electronic effects playing a minor role (12).

In this work, we further characterized these systems, conducting temperature-programmed reduction experiments and UV-Vis diffuse reflectance spectroscopy. The use of model reactions has proved to be an effective way to investigate these systems (13); hence we have tested and compared Pt, Pt-Sn, and Pt-In catalysts in three reactions: cyclohexane dehydrogenation, methylcyclopentane hydrogenolysis, and *n*-heptane conversion. These reactions are adequate to probe the nature of the active phase of these catalysts, as they demand active sites of different nature, both in terms of ensemble size or due to the need for bifunctional mechanisms including metal sites and support acid sites. The cyclohexane reaction is an insensitive to structure reaction which demands small clusters of platinum (14–16). The methylcyclopentane hydrogenolysis is sensitive to the surface structure in terms of the position of ring cleavage (17). The conversion of *n*-heptane was used to model the reactions that may occur in the industrial process. There is a competition between hydrogenolysis, hydrocracking, dehydrocyclization, and isomerization reactions (18–19). Some of these reactions occur on metallic sites, some take place on acid sites, while others require a bifunctional mechanism.

<sup>1</sup> To whom correspondence should be addressed.

The obtained results allowed us to identify the similarities and differences between Sn and In as promoters.

## EXPERIMENTAL

### Preparation of Catalysts

Al<sub>2</sub>O<sub>3</sub> (Harshaw Al3996, 200m<sup>2</sup>/g) was used as the support material in this study. Pt/Al<sub>2</sub>O<sub>3</sub> catalysts were prepared by the incipient wetness technique, using an aqueous solution of H<sub>2</sub>PtCl<sub>6</sub> (Vetec), followed by drying at 393 K for 16 h, and calcination in air at 773 K for 2 h. In/Al<sub>2</sub>O<sub>3</sub> was prepared similarly with an aqueous solution of In(NO<sub>3</sub>)<sub>3</sub> (Aldrich), while an aqueous solution of SnCl<sub>2</sub> (Riedel de Haen) was used in the preparation of Sn/Al<sub>2</sub>O<sub>3</sub>.

Bimetallic Pt-In/Al<sub>2</sub>O<sub>3</sub> and Pt-Sn/Al<sub>2</sub>O<sub>3</sub> catalysts were prepared in three distinct ways:

(i) (Pt + Sn)/Al<sub>2</sub>O<sub>3</sub> and (Pt + In)/Al<sub>2</sub>O<sub>3</sub> catalysts were prepared by coimpregnation of the support with an aqueous solution containing both metallic precursors. After the impregnation, the samples were dried at 393 K for 16 h.

(ii) Reimpregnation of Pt/Al<sub>2</sub>O<sub>3</sub> catalyst after an intermediate calcination step with an In(NO<sub>3</sub>)<sub>3</sub> or SnCl<sub>2</sub> aqueous solution was used in the preparation of In + (Pt/Al<sub>2</sub>O<sub>3</sub>) or Sn + (Pt/Al<sub>2</sub>O<sub>3</sub>) catalysts, followed by drying at 393 K for 16 h.

(iii) Pt + (In/Al<sub>2</sub>O<sub>3</sub>) and Pt + (Sn/Al<sub>2</sub>O<sub>3</sub>) catalysts were prepared by reimpregnation of In/Al<sub>2</sub>O<sub>3</sub> or Sn/Al<sub>2</sub>O<sub>3</sub> samples after an intermediate calcination step, with an H<sub>2</sub>PtCl<sub>6</sub> aqueous solution, followed by the drying step.

The dried samples were ground and calcined in air at 773 K for 2 h. The prepared catalysts and their metal contents are listed on Table 1.

### Diffuse Reflectance Spectroscopy

The calcined samples were characterized at room temperature in a VARIAN model Cary 5 UV-Vis-NIR spectrophotometer equipped with a Diffuse Reflectance Accessory Praying Mantis (Harrick geometry). Before the measurements, the samples were dried at 393 K for 16 h in an oven. The diffuse reflectance spectra were collected with an integration sphere, coated with BaSO<sub>4</sub>. In order to separate the contribution from the support, the reflectance R(λ) of the sample was made proportional to the reflectance of the support, and the Kubelka–Munk function (F(R)) was calculated.

### Temperature Programmed Reduction

The methodology and apparatus of TPR can be found in Ref. (20). The precursors (1 g) were dehydrated at 393 K for 30 min, under an Ar flow, before being submitted to a reducing gas consisting of a 1.3% H<sub>2</sub> in Ar stream. The flow rate was 30 cm<sup>3</sup>/min, and the temperature could be raised to 1073 K at a heating rate of 10 K/min.

### Chemisorption

Hydrogen chemisorption was performed at the same apparatus of TPR. After reduction at 773 K, the catalyst was outgassed with an Ar gas flow at 773 K for 30 min, in order to remove any adsorbed H<sub>2</sub>. After that, the sample was cooled to room temperature and the amount of irreversibly adsorbed H<sub>2</sub> was measured by a frontal method (21). Then, the sample was outgassed with Ar at the adsorption temperature. It was exposed to a 1.5% O<sub>2</sub>/He mixture, followed by purging with Ar. The oxygen strongly adsorbed to the sample was titrated using the same procedure for measuring the irreversibly H<sub>2</sub> by the frontal method.

TABLE 1  
Chemical Composition and H<sub>2</sub> Uptake During TPR Experiments of Pt/Al<sub>2</sub>O<sub>3</sub> Catalysts

Catalyst	Composition (wt%)			TPR H <sub>2</sub> uptake <sup>a</sup> (μmol/g <sub>cat</sub> )		Amount of In <sup>0</sup> or Sn <sup>0b</sup> (%)	
	Pt	In	Sn	773 K	1073 K/973 K	773 K	1073 K/973 K
0.7% Pt/Al <sub>2</sub> O <sub>3</sub>	0.69	—	-	73.1	-	-	-
0.9% Pt/Al <sub>2</sub> O <sub>3</sub>	0.9	-	-	89.1	-	-	-
In/Al <sub>2</sub> O <sub>3</sub>	-	0.79	-	54.3	71.3	52	68
(Pt + In)/Al <sub>2</sub> O <sub>3</sub>	0.66	0.81	-	129.3	163.0	58	90
In + (Pt/Al <sub>2</sub> O <sub>3</sub> )	0.71	0.78	-	152.5	199.3	78	100
Pt + (In/Al <sub>2</sub> O <sub>3</sub> )	0.68	0.80	-	122.9	165.2	51	91
Sn/Al <sub>2</sub> O <sub>3</sub>	-	-	0.9	76.4	83.4	0.8	10
(Pt + Sn)/Al <sub>2</sub> O <sub>3</sub>	0.92	-	0.73	167.9	172.0	20	26
Sn + (Pt/Al <sub>2</sub> O <sub>3</sub> )	0.95	-	0.87	160.6	201.0	0	41
Pt + (Sn/Al <sub>2</sub> O <sub>3</sub> )	0.89	-	0.82	190.0	197.0	43	53

<sup>a</sup> H<sub>2</sub> uptake during TPR analysis with final temperatures of 773 K and 1073 K (973 K for Pt-Sn catalysts).

<sup>b</sup> Relative amount of In<sup>0</sup> or Sn<sup>0</sup> formed after reduction at 773 K and 1073 K (973 K for Pt-Sn catalysts).

### Pyridine Adsorption

Infrared spectra of adsorbed pyridine were obtained on a Perkin-Elmer model 2000 FTIR at a resolution of  $2\text{ cm}^{-1}$ . The spectra were collected after chemisorption of pyridine at the following temperatures: 423, 523, and 623 K. The samples were pressed in the form of self-supporting disks and weighed around 25 mg. The pretreatment of the catalysts consisted of reduction at 773 K for 1 h followed by evacuation at  $10^{-5}$  Torr and 773 K.

### Cyclohexane Dehydrogenation

This reaction was performed at  $10^5$  Pa in a flow microreactor. The sample (10 mg) was previously dried *in situ* under  $\text{N}_2$  flow ( $30\text{ cm}^3/\text{min}$ ) at 393 K for 30 min. Then, it was reduced under a 1.5%  $\text{H}_2/\text{N}_2$  flow at 773 K for 30 min. After the reduction step, the reactor was cooled under the  $\text{H}_2/\text{N}_2$  flow to the reaction temperature. Hydrogen (99.999%) was further purified by passage through a molecular sieve and through a filter containing a palladium catalyst. The reactant mixture was obtained by bubbling hydrogen through a saturator containing cyclohexane (99.9%) at 285 K ( $\text{H}_2/\text{C}_6\text{H}_{12} = 13.2$ ). The space velocity (WHSV)  $170\text{ h}^{-1}$ , and the temperature was varied from 520 K to 570 K. At these conditions, no mass transfer or equilibrium limitations were observed. The conversions were kept below 10%. The composition of the effluent gas phase was measured by an on-line gas chromatograph equipped with a flame ionization detector and Carbowax 20-M in a Chromosorb W column. Turnover frequencies were determined using the amount of hydrogen irreversibly adsorbed on the catalysts after reduction at 773 K.

### Methylcyclopentane Hydrogenolysis

MCP hydrogenolysis was carried out at  $10^5$  Pa and 573 K. The samples were pretreated in the same way as in the cyclohexane dehydrogenation. All the experiments were conducted with an MCP/ $\text{H}_2$  (1 : 10.5) mixture. The space velocity was  $30\text{ h}^{-1}$  and conversions were kept below 10%. The products were analyzed by a gas chromatograph equipped with a polypropyleneglycol in a Chromosorb W packed column and a flame ionization detector. The selectivities to *n*-hexane, 2-methyl-pentane, and 3-methyl-pentane were calculated according to the ratio between the molar amount of methylcyclopentane converted to a certain product and the total molar amount of methylcyclopentane converted.

### Conversion of *n*-Heptane

The *n*-heptane reaction was measured in a continuous flow mode at  $10^5$  Pa and 773 K. The samples were dried under  $\text{N}_2$  flow at 423 K for 30 min and then, reduced under a  $30\text{ cm}^3/\text{min}$ ,  $\text{H}_2$  flow for 30 min at 773 K. The reactant mixture consisted of a 16 : 1  $\text{H}_2/\text{C}_7\text{H}_{16}$  gas mixture, obtained by bubbling  $\text{H}_2$  in a saturator containing *n*-heptane

at 298 K and the space velocity used was  $9\text{ h}^{-1}$ . Effluent products were analyzed by an on line gas chromatograph equipped with a 50-m  $\text{KCl-Al}_2\text{O}_3$  capillary column. The selectivities of the several catalysts were compared after a stationary conversion was reached and the flow adjusted to obtain an iso-conversion equal to 50%. The selectivity for each range of products was calculated as the ratio between the molar amount of *n*-heptane converted to each range of products and the total molar amount of *n*-heptane converted. Therefore, the hydrogenolysis selectivity includes the conversion of *n*-heptane to methane, ethane,  $\text{C}_5$ , and  $\text{C}_6$  fractions; the hydrocracking selectivity includes the conversion of *n*-heptane to  $\text{C}_3$  and  $\text{C}_4$  fractions, the isomerization selectivity comprises the conversion of *n*-heptane to  $\text{C}_7$  isomers formed, the dehydrogenation selectivity considers the amount of *n*-heptane converted to  $\text{C}_7$  olefins, and the aromatization selectivity includes the amount of *n*-heptane converted to toluene.

## RESULTS

### Temperature Programmed Reduction

Figures 1 and 2 present the TPR profiles of the catalysts studied. The reduction profile of  $\text{Pt}/\text{Al}_2\text{O}_3$  was similar to those reported in the literature (22–24). The TPR profiles of  $\text{Pt}/\text{Al}_2\text{O}_3$  and of all the  $\text{Pt-In}/\text{Al}_2\text{O}_3$  and  $\text{Pt-Sn}/\text{Al}_2\text{O}_3$  catalysts exhibited a maximum reduction rate at 563 K, which has been related to the reduction of a oxochloroplatinum surface complex (23).  $\text{In}/\text{Al}_2\text{O}_3$  presented a broad peak, with two main regions of reduction, one at 650 K and the other at 850 K. Besides, in the case of the bimetallic catalysts, part of the reduction of  $\text{In}^{3+}$  was shifted to the range of platinum reduction (around 560 K), as shown by the increase in the area of this range of reduction, although a high temperature region of reduction was also observed.  $\text{Sn}/\text{Al}_2\text{O}_3$  also presented a broad peak, with a shoulder at 560 K, followed by a broad range of reduction. The profiles of the  $\text{Pt-Sn}/\text{Al}_2\text{O}_3$  catalysts were different from the simple superposition of  $\text{Pt}/\text{Al}_2\text{O}_3$  and  $\text{Sn}/\text{Al}_2\text{O}_3$  profiles, which were also noted by the increase on the area of the main reduction peak.

The  $\text{H}_2$  uptakes during the TPR experiments in which the final temperature was 773 K are presented in Table 1. Considering that after the calcination step the valence state of indium is  $\text{In}^{3+}$ , we could calculate that after the reduction step 52% of the indium atoms were present on a zero-valent state in the  $\text{In}/\text{Al}_2\text{O}_3$  catalyst.  $\text{In} + (\text{Pt}/\text{Al}_2\text{O}_3)$  catalyst was the only sample that presented a higher amount of  $\text{In}^0$  (78%) than  $\text{In}/\text{Al}_2\text{O}_3$ . In the case of the other bimetallic catalysts, the amount of  $\text{In}^0$  was approximately the same, ranging from 51% to 58%. Similarly, for the Sn-containing catalysts we were able to estimate that for  $\text{Sn}/\text{Al}_2\text{O}_3$  and for  $\text{Sn} + (\text{Pt}/\text{Al}_2\text{O}_3)$ , the main oxidation state was  $\text{Sn}^{2+}$ . Some formation of  $\text{Sn}^0$  was observed for  $(\text{Pt} + \text{Sn})/\text{Al}_2\text{O}_3$  and for

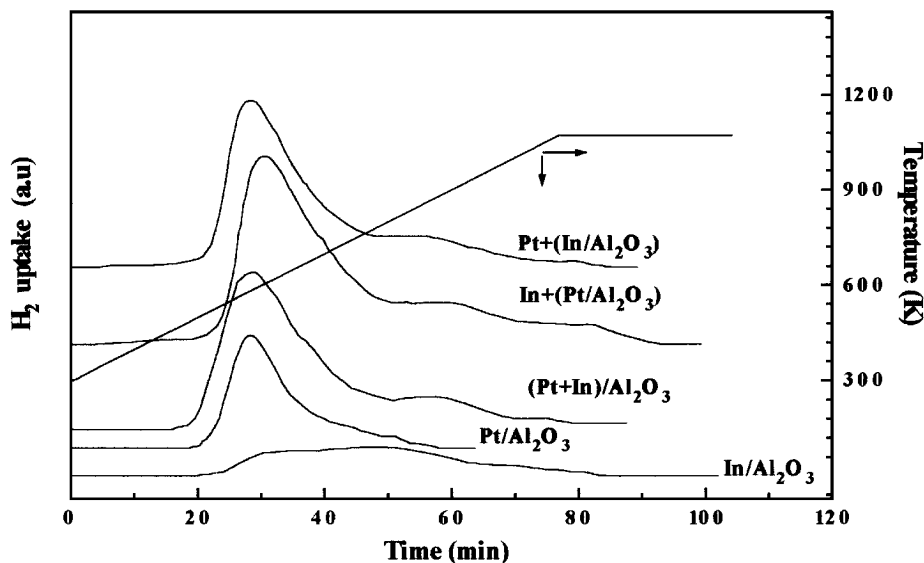


FIG. 1. Temperature-programmed reduction profiles for Pt/Al<sub>2</sub>O<sub>3</sub> and Pt-In/Al<sub>2</sub>O<sub>3</sub> catalysts.

Pt + (Sn/Al<sub>2</sub>O<sub>3</sub>) catalysts. The values presented in this work for the amount of Sn<sup>0</sup> are estimations as they suppose a homogenous reduction of Sn<sup>+4</sup> on the surface of catalysts. If there is preferential reduction of Sn atoms in direct contact with the Pt atoms, larger amounts of Sn<sup>0</sup> could be present. However, our values are similar to the ones observed by Mössbauer spectroscopy (10). The H<sub>2</sub> uptakes after the reduction at 1073 K are also listed on Table 1. The increase in the amount of In<sup>0</sup> for the bimetallic catalysts is significant

and points to a catalytic effect of platinum for the indium reduction. Pt-Sn showed similar results but on a smaller scale.

#### H<sub>2</sub> Chemisorption

The amounts of irreversibly adsorbed H<sub>2</sub>, at room temperature, on the several catalysts are shown in Table 2. The results obtained by the frontal method are in good

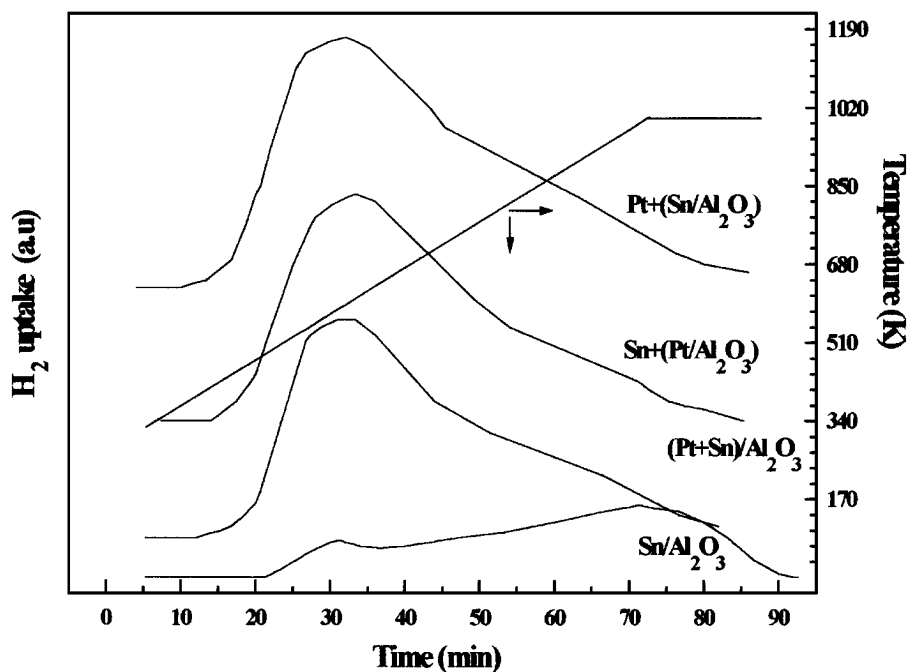


FIG. 2. Temperature-programmed reduction profiles for Pt/Al<sub>2</sub>O<sub>3</sub> and Pt-Sn/Al<sub>2</sub>O<sub>3</sub> catalysts.

TABLE 2  
H<sub>2</sub> Chemisorption and H<sub>2</sub>/O<sub>2</sub> Titration on Pt/Al<sub>2</sub>O<sub>3</sub>  
Catalysts at 300 K

Catalyst	H <sub>2</sub> uptake <sup>a</sup> (μmoles/g <sub>cat</sub> )	H/Pt <sup>b</sup>	Titration <sup>c</sup> (μmoles/g <sub>cat</sub> )
0.7% Pt/Al <sub>2</sub> O <sub>3</sub>	20.4	1.1	60.1
0.9% Pt/Al <sub>2</sub> O <sub>3</sub>	21.4	0.93	52.0
(Pt + In)/Al <sub>2</sub> O <sub>3</sub>	6.0	0.35	23.6
In + (Pt/Al <sub>2</sub> O <sub>3</sub> )	11.1	0.61	40.0
Pt + (In/Al <sub>2</sub> O <sub>3</sub> )	9.7	0.56	28.1
(Pt + Sn)/Al <sub>2</sub> O <sub>3</sub>	15.1	0.64	44.6
Sn + (Pt/Al <sub>2</sub> O <sub>3</sub> )	13.8	0.57	41.5
Pt + (Sn/Al <sub>2</sub> O <sub>3</sub> )	15.8	0.69	54.3

<sup>a</sup> Irreversible H<sub>2</sub> uptake at 300 K.

<sup>b</sup> Ratio between the number of hydrogen atoms irreversibly adsorbed and total number of platinum atoms per gram of catalyst.

<sup>c</sup> Irreversible H<sub>2</sub> uptake after exposing the sample to a He/O<sub>2</sub> flow and purging with Ar.

agreement to the ones measured by the static method (12). The presence of indium or tin markedly decreased the amount of adsorbed H<sub>2</sub>. This behavior has also been observed for other bimetallic platinum-based catalysts, like Pt-Sn (5), Pt-Ge (25), and Pt-Sb (26). This decrease was higher for the coimpregnated catalyst. The results of H<sub>2</sub>/O<sub>2</sub> titration for Pt/Al<sub>2</sub>O<sub>3</sub> and Pt + (In/Al<sub>2</sub>O<sub>3</sub>) are in good agreement to the stoichiometry proposed by Benson and Boudart (27), while an excess of H<sub>2</sub> uptake is observed for (Pt + In)/Al<sub>2</sub>O<sub>3</sub> and Pt + (In/Al<sub>2</sub>O<sub>3</sub>) catalysts.

#### UV-Vis Diffuse Reflectance Spectroscopy (DRS)

The Kubelka-Munk plots obtained for all the catalysts are shown in Fig. 3. All the samples showed similar spectra with a band at 340 nm<sup>-1</sup>. This band was assigned by Lieske

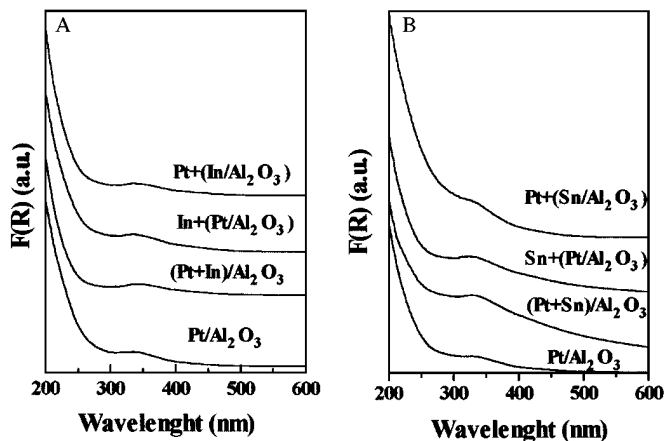


FIG. 3. DRS-UV-Vis spectra of: (A) Pt-In/Al<sub>2</sub>O<sub>3</sub> catalysts; (B) Pt-Sn/Al<sub>2</sub>O<sub>3</sub> catalysts.

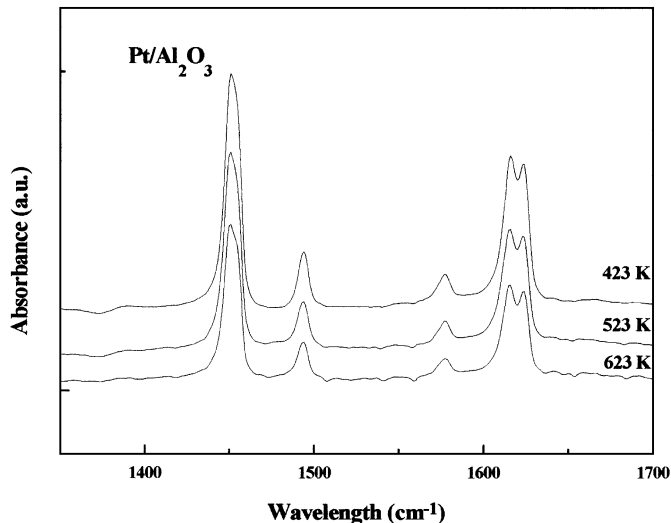


FIG. 4. Infrared spectra of adsorbed pyridine on Pt/Al<sub>2</sub>O<sub>3</sub> catalysts.

*et al.* (29) to the [PtO<sub>x</sub>Cl<sub>y</sub>]<sub>s</sub> surface complex coordinated to water, due to the fact that the samples were not dried *in situ*.

#### Pyridine Adsorption

Figures 4, 5, and 6 present the infrared spectra of adsorbed pyridine on the monometallic and coimpregnated bimetallic catalyst, while Table 3 lists the integration of bands at 1453 cm<sup>-1</sup> related to Lewis acid sites. The amount of Lewis sites was maximum for Pt/Al<sub>2</sub>O<sub>3</sub> and decreased after the addition of tin or indium. In fact, (Pt-Sn)/Al<sub>2</sub>O<sub>3</sub> showed the lowest acidity and (Pt-In)/Al<sub>2</sub>O<sub>3</sub> presented an intermediate behavior. These results were similar for all temperature ranges of our measurements.

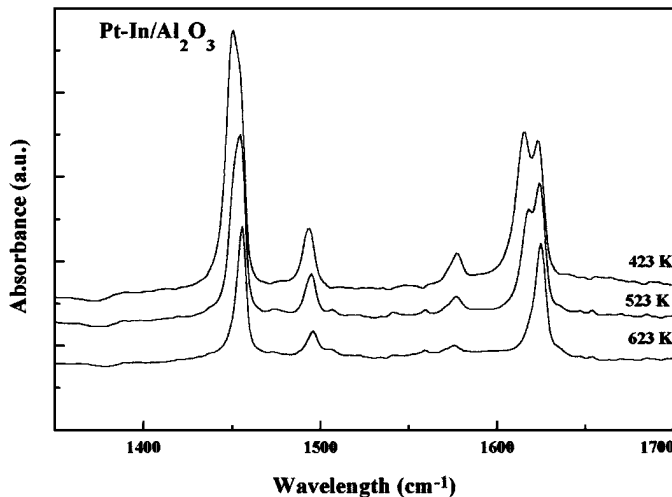


FIG. 5. Infrared spectra of adsorbed pyridine on Pt-In/Al<sub>2</sub>O<sub>3</sub> catalysts.

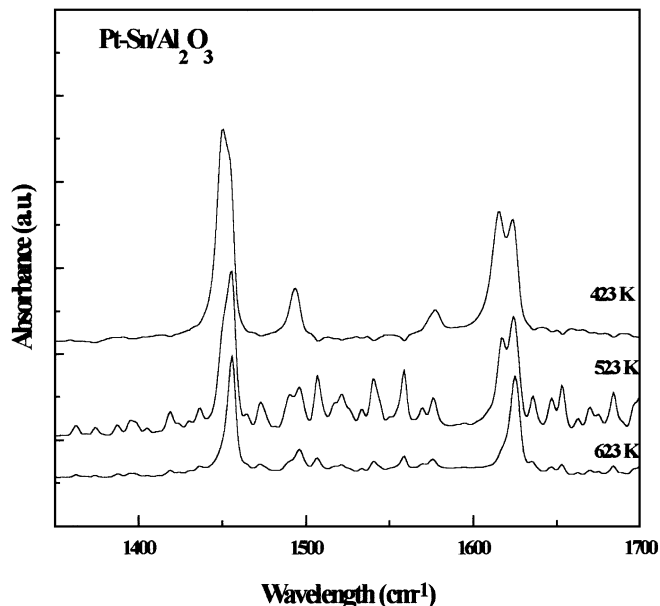


FIG. 6. Infrared spectra of adsorbed pyridine on Pt-Sn/Al<sub>2</sub>O<sub>3</sub> catalysts.

### Cyclohexane Dehydrogenation

Benzene was the only product observed for all the catalysts, and no deactivation was detected during the period of measurement (ca 4 h). Monometallic Sn/Al<sub>2</sub>O<sub>3</sub> and In/Al<sub>2</sub>O<sub>3</sub> were not active in the reaction conditions used. A summary of the results obtained is listed in Table 4. The presence of the second metal decreased the dehydrogenation activity. Besides, this decrease was proportional to the decrease in the H<sub>2</sub> chemisorption uptake so that the turnover frequency of the reaction remained practically constant, with an average value equal to 1.0 s<sup>-1</sup> with a standard deviation of 0.2 s<sup>-1</sup>. Representative Arrhenius plots are shown in Figs. 7 and 8. The apparent activation energy of the reaction was not affected significantly by the presence of the second metal. The average value obtained was 24 ± 2 kcal/mol.

### Methylcyclopentane Hydrogenolysis

Table 5 lists the activity and selectivity results for the methylcyclopentane hydrogenolysis. Sn and In promoters

TABLE 3  
Acidity of Pt/Al<sub>2</sub>O<sub>3</sub> Catalysts

Catalyst	Lewis acid sites (A.U.) <sup>a</sup>		
	423 K	523 K	623 K
Pt/Al <sub>2</sub> O <sub>3</sub>	4.08	2.69	1.69
(Pt + In)/Al <sub>2</sub> O <sub>3</sub>	3.76	2.16	1.21
(Pt + Sn)/Al <sub>2</sub> O <sub>3</sub>	3.04	1.63	0.89

<sup>a</sup> Area of 1450 cm<sup>-1</sup> infrared absorption band of chemisorbed pyridine.

TABLE 4  
Cyclohexane Dehydrogenation over Pt/Al<sub>2</sub>O<sub>3</sub> Catalysts  
(P = 1 atm H<sub>2</sub>/C<sub>6</sub>H<sub>12</sub> = 13.2)

Catalyst	Initial rate at 543 K (10 <sup>-3</sup> mol/h/g <sub>cat</sub> )	TOF <sup>a</sup> (s <sup>-1</sup> )	E <sub>a</sub> <sup>b</sup> (kcal/mol)
0.7% Pt/Al <sub>2</sub> O <sub>3</sub>	179.5	1.2	27
0.9% Pt/Al <sub>2</sub> O <sub>3</sub>	161.5	1.0	24
(Pt + In)/Al <sub>2</sub> O <sub>3</sub>	35.0	0.8	27
In + (Pt/Al <sub>2</sub> O <sub>3</sub> )	51.8	0.7	25
Pt + (In/Al <sub>2</sub> O <sub>3</sub> )	79.8	1.1	24
(Pt + Sn)/Al <sub>2</sub> O <sub>3</sub>	142.6	1.3	23
Sn + (Pt/Al <sub>2</sub> O <sub>3</sub> )	97.5	1.1	23
Pt + (Sn/Al <sub>2</sub> O <sub>3</sub> )	128.5	1.1	22

<sup>a</sup> Turnover frequencies at 543 K.

<sup>b</sup> Apparent activation energy.

caused a decrease both in the hydrogenolysis rate and in the turnover frequency. The decrease in turnover frequencies was more intense for the Pt-In/Al<sub>2</sub>O<sub>3</sub> catalysts, for which the decrease in TOF ranged from three- to sevenfold. In the case of Pt-Sn/Al<sub>2</sub>O<sub>3</sub>, the decrease in TOF was around twofold.

The selectivity distribution was close to the statistical distribution of products with the ratio between the selectivity to 2-methylpentane and the selectivity to 3-methylpentane (R<sub>1</sub>) near 2, and the ratio between the selectivity to n-hexane and the selectivity to 2-methylpentane (R<sub>2</sub>)

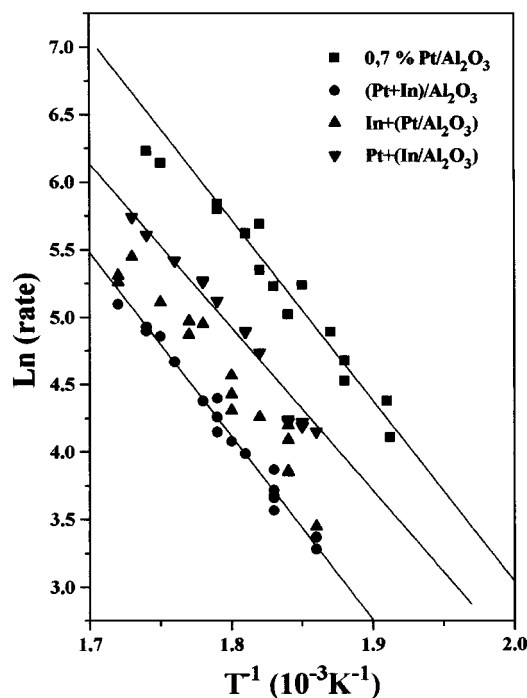


FIG. 7. Arrhenius plots for the cyclohexane dehydrogenation on Pt-In/Al<sub>2</sub>O<sub>3</sub> catalysts, p<sub>H2</sub>/p<sub>C6H12</sub> = 13.2 (P = 1 atm).

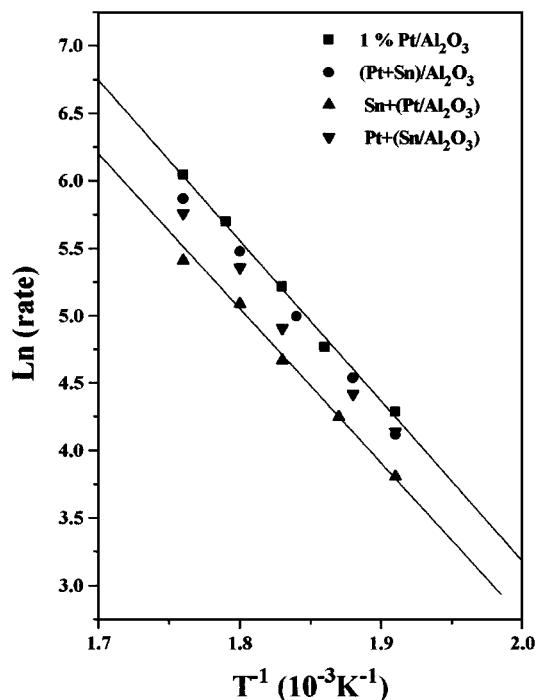


FIG. 8. Arrhenius plots for the cyclohexane dehydrogenation on Pt-Sn/Al<sub>2</sub>O<sub>3</sub> catalysts,  $p_{H_2}/p_{C_6H_{12}} = 13.2$  ( $P = 1$  atm).

around 1. For the Sn + (Pt/Al<sub>2</sub>O<sub>3</sub>) the selectivity to *n*-hexane was slightly lower than expected for a nonselective distribution.

### *n*-heptane Conversion

The effect of Sn and In on the stability and activity of Pt/Al<sub>2</sub>O<sub>3</sub> catalysts in the *n*-heptane conversion is shown in Figs. 9 and 10. It can be noted that the presence of pro-

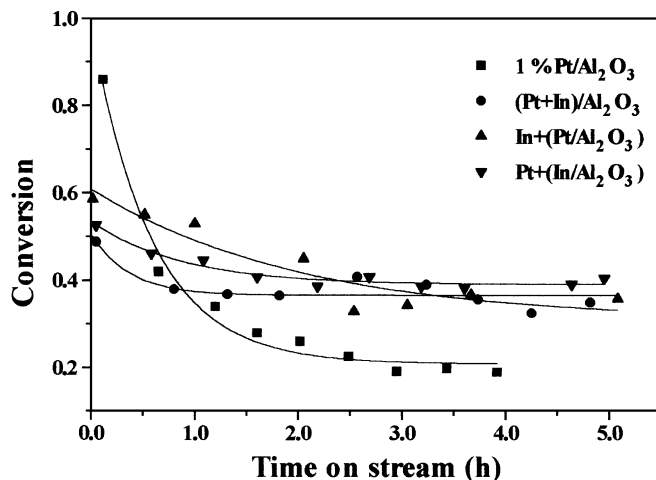


FIG. 9. Conversion of *n*-heptane on Pt-In/Al<sub>2</sub>O<sub>3</sub> catalysts at 773 K and 1 atm,  $p_{H_2}/p_{C_7H_{16}} = 16$ .

motors caused a decrease in the initial activity, but bimetallic catalysts showed better stabilities than the monometallic catalyst. Pt-In/Al<sub>2</sub>O<sub>3</sub> catalysts showed similar stationary conversions, independently of the sequence of In addition. The sequence of Sn addition had a certain influence for Pt-Sn/Al<sub>2</sub>O<sub>3</sub> catalysts; (Pt + Sn)/Al<sub>2</sub>O<sub>3</sub> and Pt + (Sn/Al<sub>2</sub>O<sub>3</sub>) presented similar activities while a lower activity was observed for Sn + (Pt/Al<sub>2</sub>O<sub>3</sub>).

The product distribution obtained in the *n*-heptane conversion for the different catalysts at an isoconversion of 50% is listed in Table 6. The addition of Sn and In to Pt/Al<sub>2</sub>O<sub>3</sub> catalysts decreased the formation of hydrogenolysis and hydrocracking products and intensified the formation of olefins and/or toluene. In fact, there was not any formation of hydrocracking and hydrogenolysis products for the Sn + (Pt/Al<sub>2</sub>O<sub>3</sub>) catalyst. The selectivities

TABLE 5

### Methylcyclopentane Hydrogenolysis over Pt/Al<sub>2</sub>O<sub>3</sub> Catalysts at 573 K

Catalyst	Initial rate (mmol/h/g <sub>cat</sub> )	TOF (10 <sup>-2</sup> s <sup>-1</sup> ) <sup>a</sup>	<i>n</i> C <sub>6</sub> <sup>b</sup> (%)	2MP <sup>c</sup> (%)	3MP <sup>d</sup> (%)	R <sub>1</sub> <sup>e</sup>	R <sub>2</sub> <sup>f</sup>
0.9%Pt/Al <sub>2</sub> O <sub>3</sub>	6.3	4.1	33	42	25	1.7	0.8
(Pt + In)/Al <sub>2</sub> O <sub>3</sub>	0.25	0.6	35	44	21	2.1	0.8
In + (Pt/Al <sub>2</sub> O <sub>3</sub> )	0.64	0.8	34	39	27	1.4	0.9
Pt + (In/Al <sub>2</sub> O <sub>3</sub> )	1.1	1.5	33	42	25	1.7	0.8
(Pt + Sn)/Al <sub>2</sub> O <sub>3</sub>	2.6	2.4	30	43	27	1.6	0.7
Sn + (Pt/Al <sub>2</sub> O <sub>3</sub> )	2.2	2.5	25	52	23	2.3	0.44
Pt + (Sn/Al <sub>2</sub> O <sub>3</sub> )	2.3	2.0	32	41	27	1.5	0.8

Note.  $P = 1$  atm,  $H_2/MCP = 10.5$ .

<sup>a</sup>Turnover frequency at 573 K.

<sup>b</sup>Selectivity to *n*-hexane.

<sup>c</sup>Selectivity to 2-methylpentane.

<sup>d</sup>Selectivity to 3-methyl pentane.

<sup>e</sup>2MP/3MP ratio.

<sup>f</sup> $nC_6/2MP$  ratio.

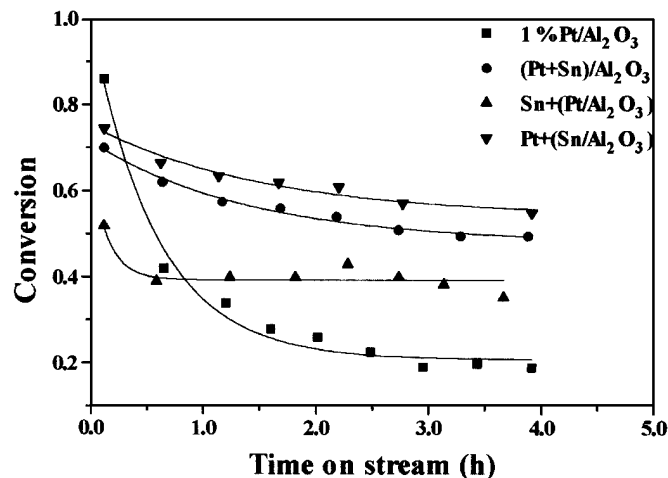


FIG. 10. Conversion of *n*-heptane on Pt-Sn/Al<sub>2</sub>O<sub>3</sub> catalysts at 773 K and 1 atm,  $p_{H_2}/p_{C_7H_{16}} = 16$ .

TABLE 6  
Selectivity for *n*-Heptane Conversion at 773 K  
on Pt/Al<sub>2</sub>O<sub>3</sub> Catalysts

Catalyst	Hydrog. <sup>a</sup>	Hydrocrack. <sup>b</sup>	C <sub>7</sub> olef <sup>c</sup>	Tol. <sup>d</sup>	Isom. <sup>e</sup>	R <sup>f</sup>
0.9% Pt/Al <sub>2</sub> O <sub>3</sub>	32	13	17	32	6	1.9
(Pt + In)/Al <sub>2</sub> O <sub>3</sub>	8	4	24	57	7	2.4
In + (Pt/Al <sub>2</sub> O <sub>3</sub> )	9	4	40	38	9	0.9
Pt + (In/Al <sub>2</sub> O <sub>3</sub> )	7	3	39	43	8	1.1
(Pt + Sn)/Al <sub>2</sub> O <sub>3</sub>	4	2	44	23	27	0.5
Sn + (Pt/Al <sub>2</sub> O <sub>3</sub> )	-	-	24	56	20	2.3
Pt + (Sn/Al <sub>2</sub> O <sub>3</sub> )	1	1	54	30	14	0.6

Note. *P* = 1 atm; H<sub>2</sub>/C<sub>7</sub>H<sub>16</sub> = 16.

<sup>a</sup>Selectivity to hydrogenolysis products.

<sup>b</sup>Selectivity to hydrocracking products.

<sup>c</sup>Selectivity to C<sub>7</sub> olefins.

<sup>d</sup>Selectivity to toluene.

<sup>e</sup>Selectivity to *n*-heptane isomers.

<sup>f</sup>Ratio between the selectivity to toluene and the selectivity to olefins.

for isomerization products observed on Pt-Sn/Al<sub>2</sub>O<sub>3</sub> catalysts were higher than those observed for Pt/Al<sub>2</sub>O<sub>3</sub> and Pt-In/Al<sub>2</sub>O<sub>3</sub> samples. It is also interesting to compare the variation of the ratio (*R*) of the toluene production to the olefin formation. Compared to the value obtained for Pt/Al<sub>2</sub>O<sub>3</sub>, (Pt + In)/Al<sub>2</sub>O<sub>3</sub> and Sn + (Pt/Al<sub>2</sub>O<sub>3</sub>) samples presented similar values while the other bimetallic catalysts showed lower values. Figure 11 displays the selectivities towards three reaction pathways as a function of the normalized acidity. Hydrocracking showed an increase with the acidity density, while isomerization was more important for the catalyst with the lowest acidity. On the other hand,

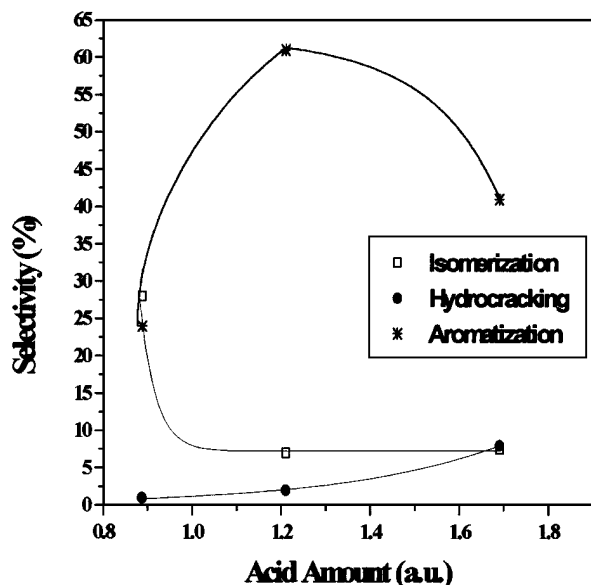


FIG. 11. Selectivity of *n*-heptane conversion as a function of the acidity of the catalysts.

aromatic products were mainly observed at intermediate acidity of the (Pt-In)/Al<sub>2</sub>O<sub>3</sub> catalyst.

## DISCUSSION

The TPR profile of In/Al<sub>2</sub>O<sub>3</sub> with two main regions of reduction indicates two different indium species fixed on alumina, as was observed for tin (5). The low and high temperature peaks are probably related to In<sub>2</sub>O<sub>3</sub> weakly or strongly stabilized on the Al<sub>2</sub>O<sub>3</sub>, respectively. After reduction at 773 K, there is the formation of In<sup>0</sup>, but there is still some In<sup>3+</sup> stabilized by the formation of an In<sup>3+</sup>-alumina surface complex.

An interaction between Pt and In can be proposed from the profiles of reduction of the bimetallic catalysts, as they are not equal the sum of the TPR profiles of the monometallic catalysts. There is a shift of part of the reduction of In<sup>3+</sup> or Sn<sup>4+</sup> to the range of Pt<sup>4+</sup> reduction, as observed by the increase in the area of the peak around 560 K for the bimetallic catalysts. Similar results were reported in the literature for the TPR profiles of bimetallic systems like Pt-Sn (5,6) and Pt-Ge (25). Platinum is able to activate H<sub>2</sub>, which reduces the precursor of the second metal (5). On the other hand, the peak around 800 K was also present on the bimetallic samples, indicating that some of the indium atoms were stabilized on the surface of alumina.

The H<sub>2</sub> uptakes during the reduction at 773 K implied the formation of either In<sup>0</sup> particles or Pt-In bimetallic clusters. There is no direct relation between the decrease in the amount of adsorbed H<sub>2</sub> and the amount of In in zero-valent state. This suggests there were some isolated In<sup>0</sup> atoms, which were not forming bimetallic clusters with platinum.

The H<sub>2</sub>/O<sub>2</sub> titration results agrees fairly well with the H<sub>2</sub> chemisorption results. Although In is able to adsorb O<sub>2</sub> (29), H<sub>2</sub> titrates only O<sub>2</sub> adsorbed on Pt. This has also been observed for Pt-Sn/Al<sub>2</sub>O<sub>3</sub> catalysts, where it was found that after one O<sub>2</sub>/H<sub>2</sub> cycle the subsequent O<sub>2</sub> adsorption was largely specific to platinum sites (30).

The DRS experiments showed the interaction between Pt and In and Pt-Sn takes place during the reduction step, since the surface platinum complex was not modified after calcination. All the samples presented similar Kubelka-Munk plots in these experiments, leading to the conclusion that the platinum surface complex precursor is the same for monometallic and bimetallic catalysts. Baronetti *et al.* (31) reported the formation of a Pt-Sn complex when Pt-Sn/Al<sub>2</sub>O<sub>3</sub> was prepared by coimpregnation. Our results, however, demonstrate that the interaction between the active metal and promoter does not need to take place during the impregnation step in order to form bimetallic particles.

The dehydrogenation of cyclohexane occurs on small metallic clusters via a  $\pi$ -allylic adsorption mechanism in which cyclohexane is successively dehydrogenated on the catalyst surface (32, 33). This reaction is considered as



structure insensitive and can be used as a measure of the number of metal surface sites (14–16). Therefore, the decrease in the initial rate caused by the addition of the promoters is consistent with the decrease in the platinum adsorption capacity as measured by hydrogen chemisorption. This effect has already been reported for several promoters added to Pt/Al<sub>2</sub>O<sub>3</sub> catalysts (34,35). The dehydrogenation activity was directly proportional to the irreversible hydrogen uptake, so that the turnover frequency was constant.

The apparent activation energy was not influenced by the addition of promoters. The slow step of reaction was not changed by the presence of Sn or In. The activation energy values obtained are also indicative that the reaction was performed under true kinetic conditions.

From these results, it is possible to conclude that for a reaction that demands small metallic ensembles, the presence of In and Sn does not modify the turnover frequency; i.e., there is not any change in the intrinsic catalytic properties of the platinum surface atoms which are not blocked by the promoter.

Methylcyclopentane hydrogenolysis is a structure-sensitive reaction, whose product distribution depends on the metal particle size (17). In the case of small platinum particles, the reaction is nonselective, forming 20% 3-methylpentane, 40% 2-methylpentane, and 40% *n*-hexane. This distribution is identical to the statistical probability, considering the possible positions of ring cleavage. For larger platinum particles, the ring opening is selective, producing 33% 3-methylpentane and 67% 2-methylpentane, while the formation of *n*-hexane is excluded. It has been suggested that selective ring opening occurs via  $\alpha,\alpha,\beta,\beta$  tetra-adsorbed species, followed by bond breaking between the  $\alpha$  and  $\beta$  atoms, suppressing the *n*-hexane formation. On the other hand, nonselective ring cleavage was supposed to occur via  $\alpha,\alpha,\beta$  tri-adsorbed species bound to edge and corner atoms (36). Páal and Tètényi (26) suggested that the C<sub>5</sub> ring adsorbs in a flat mode, parallel to the surface, as an intermediate of the selective mechanism. Krammer and Zuegg (38) proposed an *adlineation mechanism*, where the methylcyclopentane reacts on the surface of platinum crystallites to form 2-methylpentane or 3-methylpentane, while the formation of *n*-hexane occurs only on the platinum-support interface, explaining the particle size dependence. Later, this model was refined; the *n*-hexane formation on the metal-support interface was explained by the fact that platinum atoms in contact with the support are considered with a positive partial charge, due to electron transfer from the platinum atoms to the support (39).

The catalysts tested in this work showed only a nonselective product distribution, even for the bimetallic catalysts for which the H/Pt ratio was low. In fact, for a 10% Pt/Al<sub>2</sub>O<sub>3</sub> catalyst which presented a selective product distribution, the addition of Sn favored the nonselective distribution

(40). This was explained by the dilution of platinum particles by Sn. Similar results were obtained for Pt-Cu/SiO<sub>2</sub> (41). Assuming that the mechanism for the formation of *n*-hexanes at the metal-support interface due to electron transfer from the metal to the support is correct, a possible electron transfer from Sn and In to platinum would cause a decrease in the selectivity to *n*-hexane. However, this was not observed, indicating that the main mechanism of Sn and In promotion is geometric, in agreement with CO-adsorbed infrared and adsorption calorimetric experiments performed (12).

The lower formation of *n*-hexane observed for the Sn + (Pt/Al<sub>2</sub>O<sub>3</sub>) catalyst can be explained by a heterogeneous distribution of particle sizes in this sample. This hypothesis is consistent with CO adsorbed infrared measurements (12) for which this catalyst presented a small increase in the linearly bound CO adsorption frequency.

The bimetallic catalysts also presented a decrease in the turnover frequency (TOF) for MCP hydrogenolysis, which was more intense for the Pt-In catalysts. The TOF change was relatively small, as there was not a change in order of magnitude for the catalysts investigated. For cyclopentane hydrogenolysis, the addition of Ge to Pt/Al<sub>2</sub>O<sub>3</sub> caused a 200-fold decrease in TOF (25), while cyclopropane hydrogenolysis was considered a structure-insensitive reaction (42), implying the change in TOF for hydrogenolysis with the metallic ensemble size depends on the molecule being investigated. Unfortunately, it was not possible to calculate TOF values for the methylcyclopentane hydrogenolysis studies reported in the literature so that we could compare our results.

The results for *n*-heptane conversion demonstrated the positive features of Sn and In addition to Pt/Al<sub>2</sub>O<sub>3</sub> catalysts. The bimetallic catalysts showed a better stability, as compared to the monometallic catalyst. Furthermore, the selectivity for the so-called nondestructive reactions, such as the olefin and aromatic formation, was improved by the presence of Sn and In with further inhibition of hydrogenolysis and hydrocracking reactions. Similar results have been observed before (6,43–44) and can be explained by the different demands for platinum clusters by the several reactions that can take place in this reaction system. The hydrogenolysis reactions demand large Pt ensembles. As the addition of promoters decrease the size of the ensembles, hydrogenolysis reactions are suppressed. On the other hand, the stability is improved due to the fact that coke precursors are relatively large and also demand large ensembles for adsorption. The promoter presence hinders the adsorption of these molecules on the metal atoms, and the coke precursors are drained to the support surface, leaving the metal surface available for reaction. In addition, Querini and Fung (45) have shown an increase in the surface concentration of hydrogen on Pt-Re/Al<sub>2</sub>O<sub>3</sub>, as compared to the Pt/Al<sub>2</sub>O<sub>3</sub> catalyst. Thus, this effect could also

improve the catalyst stability with the addition of In and Sn to the platinum surface.

Although the bimetallic catalysts presented the same trend in terms of a higher selectivity to dehydrogenation and dehydrocyclization products, there were some differences in the selectivity distribution for the several catalysts. The balance between the several competitive pathways taking place in the *n*-heptane conversion is different for each sample.

The higher selectivity for isomerization on the Pt-Sn samples is consistent with previous results (46). It was proposed that the addition of tin reduces the acid sites that promote hydrocracking reactions, forming sites which are selective for the isomerization of olefins. This feature was not observed on the Pt-In/Al<sub>2</sub>O<sub>3</sub> samples for which the isomer formation was comparable to the ones obtained with Pt/Al<sub>2</sub>O<sub>3</sub>. However, the Pt/Al<sub>2</sub>O<sub>3</sub> catalyst showed higher hydrocracking selectivity than (Pt-In)/Al<sub>2</sub>O<sub>3</sub>, which indicates the highest acidity density on the monometallic catalyst, as confirmed by pyridine adsorption. Thus, the (Pt-In)/Al<sub>2</sub>O<sub>3</sub> catalyst showed an intermediate acidity which, together with the metallic activity, produced the highest selectivity towards aromatics.

### SUMMARY

In this work, platinum-tin and platinum-indium catalysts were investigated. The TPR and H<sub>2</sub> chemisorption results pointed to a multiple scenario for states of In and Sn in these catalysts. Part of the promoter atoms are interacting strongly with the support forming Sn<sup>2+</sup>/Al<sub>2</sub>O<sub>3</sub> or In<sup>3+</sup>/Al<sub>2</sub>O<sub>3</sub>. Another fraction of the promoter atoms are interacting with the platinum atoms, forming bimetallic clusters. The remainder of the promoter atoms, are isolated zero-valent atoms, interacting weakly with the support.

When model reactions were studied to differentiate the effect of Sn and In on the catalytic properties of Pt/Al<sub>2</sub>O<sub>3</sub> catalysts, it was demonstrated that the catalyst performance depends on both the chemical nature of the chemical reaction, as well as on the promoters employed. Initially, it is necessary to separate two large reaction groups: reactions that take place only on the metallic phase, and the hydrocarbon conversions for which there are reactions that occur on the metallic phase and reactions that take place on the acidic sites of the support. For those insensitive to the structure reactions, such as the cyclohexane dehydrogenation, the promoter does not change the turnover frequency, with the change in the catalytic activity being proportional to the number of exposed surface platinum atoms. In the case of reactions that demand larger metal ensembles, the promoter presence causes a decrease in the turnover frequency. The intensity of this decrease depends upon the molecule being reacted. The changes observed for *n*-butane hydrogenolysis (12) were much larger than

the ones obtained for methylcyclopentane hydrogenolysis in this work. On the other hand, the addition of In was more effective on the decrease of the hydrogenolysis activity than Sn, which was consistent to previous adsorbed CO infra-red spectroscopy results (12).

In the case of reactions for which a bifunctional mechanism can occur, as the *n*-heptane conversion, it is necessary to consider the support modifications and the competition between the several reactions, besides the metallic-phase changes. The addition of Sn or In to Pt/Al<sub>2</sub>O<sub>3</sub> improved its selectivity to nondestructive reactions such as *n*-heptane dehydrogenation and aromatization, and its stability. A difference between Sn and In was that Sn promoted an increase in the selectivity for isomerization products. In the case of In-promoted catalysts the selectivity for isomerization was low, indicating that if the presence of Sn and In blocked acid sites of the support that are responsible for hydrocracking reactions, the presence of Sn generated acid sites that are active for isomerization. The different selectivities observed for the different preparation methods pointed to the complexity of the optimization of bimetallic catalyst preparation.

### REFERENCES

1. Sinfelt, J. H., "Bimetallic Catalysts: Discoveries, Concepts and Applications." Wiley, New York, 1983.
2. Ponc, V., *Adv. Catal.* **32**, 149 (1983).
3. Verbeek, H., and Sachtler, W. M. H., *J. Catal.* **25**, 350 (1972).
4. Abrevaya, H., and Imai, T., U.S. Patent 4,608,360 (1986).
5. Lieske, H., and Völter, J., *J. Catal.* **90**, 96 (1984).
6. Dautzenberg, F. M., Helle, J. N., Biloen, P., and Sachtler, W. M. H., *J. Catal.* **63**, 119 (1980).
7. Baronetti, G. T., De Miguel, S. R., Scelza, O. A., Fritzler, M. A., and Castro, A. A., *Appl. Catal.* **19**, 77 (1985).
8. Burch, R., *J. Catal.* **71**, 348 (1981).
9. Balakrishnan, K., and Schwank, J., *J. Catal.* **127**, 287 (1991).
10. Hobson, M. C., Jr., Goresch, S. L., and Khare, G. P., *J. Catal.* **142**, 641 (1993).
11. Loc, L. C., Thoang, H. S., Gaidai, N. A., and Kiperman, S. L., "Proceedings of 10th International Congress on Catalysis, Budapest, 1992, part C," p. 2277. Elsevier, Amsterdam, 1993.
12. Passos, F. B., Schmal, M., and Vannice, M. A., *J. Catal.* **160**, 106 (1996).
13. Páal, Z., *Catal. Today* **2**, 595 (1988).
14. Poltorak, O. M., and Boronin, V. S., *Zhur. Fis. Khim.* **40**, 2761 (1966).
15. Guenin, M., Breyse, M., Fréty, R., Tifouti, K., Marecot, P., and Barbier, J., *J. Catal.* **105**, 144 (1987).
16. Kraft, M., and Spindler, R. M., in "Proceedings of 4th International Congress on Catalysis, Moscow, 1968." Vol. 3, p. 1252.
17. Gault, F. G., *Adv. Catal.* **30**, 1 (1981).
18. Gates, B., Katzer, J., and Schuit, G. C. A., "Chemistry of Catalytic Processes." Mc-Graw-Hill, New York, 1979.
19. McVicker, G. B., Collins, P. J., and Ziemiack, J. J., *J. Catal.* **74**, 156 (1982).
20. Noronha, F. B., Primet, M., Fréty, R., and Schmal, M., *Appl. Catal.* **78**, 125 (1991).
21. Blanchard, G., Charcosset, H., Forissier, M., Matray, F., and Tournayan, L., *J. Chromatogr. Sci.* **20**, 369 (1982).
22. Yao, H. C., Sieg, M., and Plummer, H. K., *J. Catal.* **59**, 365 (1978).

23. Lieske, H., Lietz, G., Spindler, H., and Völter, J., *J. Catal.* **81**, 8 (1983).
24. Wagstaff, N., and Prins, R., *J. Catal.* **59**, 434 (1983).
25. De Miguel, S. R., Correa, J., Baronetti, G. T., and Castro, A. A., *Appl. Catal.* **60**, 47 (1990).
26. Cheng, M. C., Dooley, K. M., and Price, G. L., *J. Catal.* **116**, 325 (1989).
27. Benson, J. E., and Boudart, M., *J. Catal.* **4**, 704 (1965).
28. Lietz, G., Lieske, H., Spindler, H., Hanke, W., and Völter, J., *J. Catal.* **81**, 17 (1983).
29. Dai, D-X., Zhu, F-R., Davoli, I., and Stizza, S., *Appl. Surf. Sci.* **59**, 195 (1992).
30. Zhou, Y., and Davis, S. M., *Catal. Lett.* **15**, 51 (1992).
31. Baronetti, G. T., De Miguel, S. R., Scelza, O. A., and Castro, A. A., *Appl. Catal.* **24**, 109 (1986).
32. Paál, Z., and Tétényi, P., *Nature* **267**, 234 (1987).
33. Krishnasamy, V., and Balasubramanian, K., *J. Catal.* **90**, 351 (1984).
34. Lanh, H. D., Thoang, H. S., Lieske, H., and Völter, J., *Appl. Catal.* **11**, 195 (1984).
35. Baronetti, G. T., de Miguel, S. R., Scelza, O. A., and Castro, A. A., *Appl. Catal.* **11**, 195 (1984).
36. Luck, F., Schmidt, J. L., and Maire, G., *React. Kinet. Catal. Lett.* **21**, 219 (1982).
37. Paál, Z., and Tétényi, P., *Nature* **267**, 234 (1987).
38. Krammer, R., and Zuegg, H., *J. Catal.* **85**, 530 (1984).
39. Krammer, R., and Fischbacher, M., *J. Mol. Catal.* **51**, 247 (1989).
40. Gault, F. G., Zahraa, O., Dartigues, J. M., Maire, G., Peyrot, M., Weisang, E., and Engelhardt, P. A., in "Proceedings of 7th International Congress on Catalysis, Tokyo, 1980, Part A," p. 199. Elsevier, Amsterdam, 1981.
41. De Jongste, H. C., and Ponc, V., in "Proceedings of 7th International Congress on Catalysis, Tokyo, 1980, part A," p. 186. Elsevier, Amsterdam, 1981.
42. Boudart, M., Aldag, A., Benson, J. E., Dougharty, N. A., and Harkins, C. G., *J. Catal.* **6**, 92 (1966).
43. Völter, J., in "Catalytic Hydrogenation" (L. Cerveny, Ed.) Elsevier, Amsterdam, 1986.
44. Sparks, D. E., Srinivasam, R., and Davis, B. H., *J. Mol. Catal.* **88**, 325 (1994).
45. Querini, C. A., and Fung, S. C., *J. Catal.* **141**, 389 (1993).
46. Burch, R., and Garla, L. C., *J. Catal.* **71**, 360 (1981).